# APPENDIX A

## Derivation of the Detection Sensitivity of an Astronomical Telescope

We first consider the completely general case for an arbitrary telescope, detector, and observing conditions. Next we consider the NASA-LMT in two specific operating modes as they relate to astronomy and orbital object detection.

Signal:

From first principles, the total signal electrons ( $S$ ) registering on a detector from an external source is given by:

$$S = A_{TEL} \cdot E_S \int_{BW} TE(\lambda) \cdot QE(\lambda) \cdot F_S(\lambda) d\lambda \qquad \text{(AA.a)}$$

Where:

$A_{TEL}$ = Telescope primary aperture

$E_S$ = Signal exposure time

$BW$ = Detector bandwidth

$TE(\lambda)$ = Telescope efficiency or throughput as a function of wavelength

$QE(\lambda)$ = Detector quantum efficiency as a function of wavelength

$F_S(\lambda)$ = Signal flux as a function of wavelength

$\lambda$ = Wavelength

For a point source we can rewrite $F_S(\lambda)$ in terms of apparent magnitude $m(\lambda)$:

$$F_S(\lambda) = N \cdot 10^{(-0.4 \cdot m(\lambda))} \quad \text{(AA.b)}$$

Where:

N=10,000 $\gamma / \sec cm^2 nm$ (the photon flux for 0$^{th}$ apparent magnitude)

For a diffuse source we can rewrite $F_S(\lambda)$ in terms of surface brightness $m_{SB}(\lambda)$:

$$F_S(\lambda) = N \cdot A_{PIX} 10^{(-0.4 \cdot m_{SB}(\lambda))} \quad \text{(AA.c)}$$

Where:

$A_{PIX}$ = Area of the detector or detector element ($arc\sec ond^2$)

Making the assumption that the source flux and telescope and detector response are relatively independent of wavelength over each B,V,R, or I Band optical wavelength regime, we can approximate A-1 as:

$$S = A_{TEL} \cdot BW \cdot TE \cdot QE \cdot E_S \cdot F_S \quad \text{(AA.d)}$$

Expressing in terms of the actual signal flux at the detector $S_F$:

$$S = E_S \cdot S_F \tag{AA.e}$$

Where:

$$S_F = A_{TEL} \cdot BW \cdot TE \cdot QE \cdot \cdot F_S \tag{AA.f}$$

If this signal is spread uniformly over a $n$ pixel region of the detector in units of $S_{pix}$,

we can write:

$$S = n \cdot S_{pix} = n \cdot E_{S_{pix}} \cdot S_{F_{pix}} \tag{AA.g}$$

Where:

$E_{S_{pix}} \equiv {E_S}/{\alpha}$ = Exposure time per pixel

$S_{F_{pix}} \equiv {S_F}/{\beta}$ = Source flux per pixel

$\alpha$ = exposure reduction parameter due to object motion

$\beta$ = signal flux reduction parameter due to image spread

With the constraint $n = \alpha \cdot \beta$ and $\alpha, \beta \geq 1$

Depending on the nature of the source signal, the per pixel components of signal and exposure time can vary. Equation AA.g accounts for any configuration of source and detector: static point source sampled by a single pixel, static diffuse source sampled by multiple pixels, moving source sampled by single pixels, moving diffuse source sampled by multiple pixels.

Noise:

Governed by Poisson photon counting statistics, the total noise associated with a signal detection by a CCD detector is given by:

$$N_T = \sqrt{(R_T{}^2 + S + BKG + D_T)} \qquad \text{(AA.h)}$$

Where:

$R_T$ = Total CCD read noise for all signal pixels (includes Bias noise)

$S$ = Source signal

$BKG$ = Total Background

$D_T$ = Total Thermal Dark charge

If the signal is spread evenly over $n$ pixels, and the CCD response is uniform, we can rewrite the total noise as:

$$N_T = \sqrt{n \cdot (R_{pix}{}^2 + S_{pix} + BKG_{pix} + D_{pix})} \qquad \text{(AA.i)}$$

Where:

$R_{pix}$ = CCD read noise per pixel

$S_{pix}$ = Source signal per pixel

$BKG_{pix}$ = Background per pixel

$D_{pix}$ = Thermal Dark charge per pixel

The amount of time the detector is exposed to the field is not necessarily equal to the amount of time the signal source is exposed to the detector (eg. a meteor transit during a sidereal drift scan). Rewriting the noise in terms of the total detector exposure $E_D$ and signal exposure per pixel $E_{S_{pix}}$:

$$N_T = \sqrt{n \cdot (R_{pix}{}^2 + E_{S_{pix}} \cdot S_{F_{pix}} + E_D \cdot BKG_{F_{pix}} + E_D \cdot D_{c\,pix})} \qquad \text{(AA.j)}$$

Where:

$R_{pix}$ = CCD read noise per pixel

$E_D$ = Detector exposure time

$BKG_{F_{pix}}$ = Background flux per pixel

$D_{c_{pix}}$ = Thermal Dark current per pixel

Signal-to-Noise Ratio:

The total signal-to-noise-ratio (SNR) can be expressed as the quotient of equations (AA.g) and (AA.j):

$$SNR = \frac{n \cdot E_{S_{pix}} \cdot S_{F_{pix}}}{\sqrt{n \cdot (R_{pix}{}^2 + E_{S_{pix}} \cdot S_{F_{pix}} + E_D \cdot BKG_{F_{pix}} + E_D \cdot D_{c_{pix}})}} \qquad \text{(AA.k)}$$

Since we are interested in detection limits where the signal is small, we may safely neglect the signal related component of the noise. ($S_{pix} << R^2_{pix}, BKG_{pix}$)

Simplifying, we have:

$$SNR = \frac{\sqrt{n} \cdot E_{S_{pix}} \cdot S_{F_{pix}}}{\sqrt{(R_{pix}{}^2 + E_D \cdot BKG_{F_{pix}} + E_D \cdot D_{C_{pix}})}} \qquad \text{(AA.l)}$$

Examples:

Let us consider the case of the detection sensitivity, in two operating modes of the 3 m NASA-LMT with the LSP 2K detector, $MgF_2$ coated camera head window, and the original 3 element $MgF_2$ coated corrector lens.

For all cases, the NASA-LMT and LSP 2K CCD have the following operating parameters:

Primary mirror area = $A_{TEL}$ = 70685.8 $cm^2$ (neglecting PF obscuration of 2918 $cm^2$)

CCD Array size = 2048x2048 pixels

Pixel size = 15 um

Read Noise = $R_{pix}$ =28.1 e-

Dark Current = $D_{C_{pix}}$ =0.08 e-/pix-sec

Telescope efficiency = $TE$ = 0.679

(76.6% Hg reflectivity@ V and eight $MgF_2$ surfaces @ 98.5% each)

$QE$ = ~0.35 (V Band; 500-600 nm); ~0.18 (White Light; 450-975 nm)

$BW$ = 100 nm (V Band; 500-600 nm); 525 nm (White Light; 450-975 nm)

Case 1)
Find the limiting stellar magnitude (V Band) for a sidereal drift scan with no

CCD binning (1x1).

We wish to solve equation (AA.l) for $S_{F_{pix}}$ and then use equations (AA.b) and (AA.f)

to find the corresponding limiting magnitude.

The exposure time for a zenith sidereal drift-scan is determined by the telescope latitude,

CCD array size, and plate scale.

First, the Sidereal Drift Rate (SDR) is given by:

SDR (arcseconds/sec) = $(2\pi / 86{,}160) \cdot \cos\delta \cdot 206{,}265$ (AA.m)

Where 86,160 is the number of seconds per sidereal day and 206,265 is the number of

arcseconds/radian.

At the NODO location, with latitude $\delta$ =33 degrees North, this yields:

SDR = 12.615 arcseconds/sec.

Second, the plate scale (PS) is determined by the CCD pixel size and the telescope

focal length:

$$\text{PS (arcseconds/pixel)} = 206{,}265 \cdot \left(\frac{PixelSize}{FocalLength}\right) \qquad \text{(AA.n)}$$

For the NASA-LMT with an effective (after the finite power corrective optics) focal length of 5,173.87 mm (f/1.7246) and a LSP 2K CCD pixel size of 15 um, we have:

PS = 0.598 arcseconds/pixel

Finally, the field crossing time (FCT), and hence the total exposure time, for a star transiting the FOV is given by:

$$\text{FCT} = \frac{CCDArraySize \cdot PlateScale}{SiderealDriftRate} \qquad \text{(AA.o)}$$

For the NASA-LMT and LSP 2K CCD, this yields:

FCT = 97.1 sec

Since we are drift scanning at the sidereal rate, the stellar images are static relative to the electro-optically tracking detector pixels ($\alpha$ =1), therefore:

$$\text{FCT} = E_S = E_D = E_{S_{pix}} = 97.1 \text{ sec}$$

The per pixel background flux $BKG_{F_{pix}}$ is dependent on the telescope location.

For the NODO location, the night sky background is approximately (Schneeberger et al. 1979):

NODO Sky BKG (V band) = 21.81 $magnitudes / arc\sec ond^2$

Substituting into equation (AA.c) and safely neglecting any wavelength dependence within the V band, we have (since $A_{PIX} = PS^2$ =0.36 $arc\sec ond^2$ ):

$$F_S(\lambda) = F_S = 6.797x10^{-6}\ \gamma / \sec cm^2 nm$$

Substituting into equation (AA.f), the corresponding background flux at a detector pixel is:

$BKG_{F_{pix}}$ = 11.42 e-/pix-sec

Substituting all known values into equation (AA.l):

$$SNR = 2.229\sqrt{n} \cdot S_{F_{pix}}$$

The nominal NODO seeing value is approximately 1.2 arcseconds FWHM which implies that a stellar Point Spread function (PSF) could occupy as few as 4 pixels( $n = \beta$ =4). If we use the generally accepted limiting SNR of 6.3 we find:

$S_{F_{pix}}$ =1.413 e-/pix => $S_F$ =5.653 e-

Using equation (AAf), this corresponds to a source flux $F_S$ of:

$$F_S = 3.365x10^{-6}\ \gamma / \sec cm^2 nm$$

We use equation (AA.b) to recover the limiting V apparent magnitude:

$m_V$ = 23.68

At a SNR of 10 and a PSF spread over 9 pixels ($n = \beta$ =9), corresponding to 1.8 arcsecond seeing, we obtain:

$m_V$ =22.74

V Band observations with the NASA-LMT are made through a glass filter with a bandwidth of approximately 100 nm and an average transmittance of 0.35.

This yields actual limiting magnitudes of:

$m_V$ =22.54 for 1.2 arcsecond seeing

$m_V$ =21.60 for 1.8 arcsecond seeing

These values correlate well with empirical results, some of which are given in Chapter VI.

Case 2)

Find the limiting magnitude (V Band) and detection diameter for a high-speed drift-scan of an orbital object at 800 km altitude.

Physical limitations intrinsic to the LSP 2K CCD detector require using binned pixels in order to implement a high-speed drift-scan. Binning reduces the number of pixels which must be read by combining the charge from adjacent rows (parallel binning) or columns (serial binning) into super-pixels. Since the readout electronics require a finite amount of time to digitize each pixel, the CCD surface can be read more quickly if there are fewer pixels. Excessive binning has the disadvantage, however, of increasing the background noise associated with each portion of signal. From a SNR perspective, the signal PSF and pixel (or super-pixel) size should match, although from a photometric perspective, the signal PSF should be over-sampled by a factor of two. This reduces SNR slightly, but increase photometric accuracy by reducing the effect of pixel-to-pixel sensitivity variations.

Through extensive testing, the timing equation for the LSP 2K CCD was found empirically to be given by:

$$\text{SFRT = Single Frame Read Time (sec)} = \frac{4 \cdot Delay + 10.2}{Bin} \qquad \text{(AA.p)}$$

Where:

Delay = parallel shift delay time (sec)

$Bin$ = symmetrical binning factor in which:

$$Bin = \text{serial binning}(Bin_S) = \text{parallel binning}(Bin_P)$$

To optimize high-speed drift-scan object tracking, we require that the SFRT equal the object FCT. The FCT is given by:

$$\text{FCT} = \frac{CCDArraySize \cdot PlateScale}{\varpi_{EFF}} \qquad \text{(AA.q)}$$

Where:

$\varpi_{EFF}$ = effective orbital angular velocity of object accounting for the earth's rotation

Assuming a circular orbit, the angular velocity $\varpi_{EFF}$ (radians/sec) is given by the following expressions derived from simple gravitational and centrifugal force balance and allowing for the east-west motion of the telescope due to the earth's rotation:

$$\varpi_{EFF}^2 = \varpi_{NS}^2 + \varpi_{EW}^2 \qquad \text{(AA.r)}$$

Where:

$\varpi_{NS} = \varpi_{CIRC} \cdot \sin(90 - PA)$ (north-south angular rate)

$$\varpi_{EW} = [(\varpi_{CIRC} \cdot \cos(90 - PA)) - \varpi_{Earth} \cdot \cos(LAT)]$$ (east-west angular rate)

and

$$\varpi_{CIRC} = \sqrt{\frac{GM}{H^2(H + R_E)}}$$ (angular rate for a circular orbit) (AA.s)

and

$\varpi_{Earth}$ = angular rotational velocity of the earth = 0.004178 deg/sec

PA = position angle of object motion (north = 0 degrees)

LAT = latitude of the telescope (NODO = 32.979 degrees N)

G = Gravitational constant = $6.672x10^{-11} m^3 / kg \cdot \sec^2$

M = Mass of the Earth = $5.98x10^{24} kg$

H = Orbital altitude

$R_E$ = Radius of the Earth = 6378 km

Solving for $\varpi_{EFF}$ for an object at 800 km altitude and 0 degree position angle (PA):

$\varpi_{EFF}$ = 0.6388 degrees/sec

Substituting into equation(AA.q) yields:

FCT = 0.534 sec

Since we are drift scanning at the orbital object angular rate, the stellar images are static relative to the electro-optically tracking detector pixels ($\alpha$ =1), therefore:

FCT $= E_S = E_D = E_{S_{pix}}$ = 0.534 sec

Equating FCT to SFRT and solving equation (AA.q) for the requisite minimum binning factor, we have:

$Bin$ = 16 with Delay =0.

The binning factor must be accounted in the SNR relationship (AA.l). By simply translating the per pixel definitions to per super-pixel definitions, we account for arbitrary binning:

$$SNR = \frac{\sqrt{n} \cdot E_{S_{spix}} \cdot S_{F_{spix}}}{\sqrt{(R_{spix}{}^2 + E_D \cdot BKG_{F_{spix}} + E_D \cdot D_{c_{spix}})}} \qquad \text{(AA.t)}$$

Where:

$n$ = number of super-pixels occupied by the signal

$E_{S_{spix}}$ = signal exposure per super-pixel

$S_{F_{spix}}$ = signal flux per super-pixel

$R_{spix}$ = read noise per super-pixel (= $R_{pix}$)

$BKG_{F_{spix}} = Bin_S \cdot Bin_P \cdot BKG_{F_{pix}}$ = background level per super-pixel

$D_{C_{spix}} = Bin_S \cdot Bin_P \cdot D_{C_{pix}}$ = dark current per super-pixel

As in the first example, we substitute the known quantities below into equation (AA.t):

FCT $= E_S = E_D = E_{S_{pix}} = 0.534$ sec $= E_{S_{spix}}$

$BKG_{F_{pix}} = 11.42$ e-/pix-sec (V Band)

Substituting yields:

$$SNR = 0.01099\sqrt{n} \cdot S_{F_{pix}}$$

The nominal NODO seeing value is approximately 1.2 arcseconds FWHM which implies that a stellar Point Spread function (PSF) could occupy as few as 4 un-binned pixels. This implies that the orbital object PSF should occupy only 1/16 of the area of a single 16 binned super-pixel, therefore ($n = \beta = 1$). If we use the generally accepted limiting SNR of 6.3 we find:

$S_{F_{pix}} = 573.3$ e-/pix $= S_F$

Using equation (AA.f), this corresponds to a V Band source flux $F_S$ of:

$$F_S = 3.413x10^{-4}\ \gamma / \sec cm^2 nm$$

We use equation (AA.b) to recover the limiting V apparent magnitude:

$$m_V = 18.67$$

Next let us determine the diameter on an orbital object at 800 km altitude with an apparent magnitude of $m_V = 18.67$.

Since a telescope (as a opposed to a RADAR), observes orbital debris via reflected sunlight, the flux received from the object ($F_{s_{OBJ}}$) depends on the solar flux ($F_{SUN}$) impinging on the object:

$$F_{s_{OBJ}} = F_{SUN} \cdot \frac{A \cdot (\pi \cdot (D/2)^2)}{H^2} \cdot PF \qquad \text{(AA.u)}$$

Where:

A = Bond albedo (as opposed to geometric albedo)

D = Object diameter

H = Object altitude

PF = Object phase function

Rewriting in terms of apparent magnitudes and solving for D:

$$D = \frac{2H}{\sqrt{\pi \cdot A \cdot PF}} \cdot 10^{(-0.2 \cdot (m_{OBJ} - m_{SUN}))} \quad \text{(AA.v)}$$

Where:

$m_{SUN}$ = -26.74 (V Band)

For this example we will use the mean optical albedo <A> of 0.1 derived from extensive optical observations of orbital debris objects and comparison with catalogued radar cross-sections. (Henize et al. 1993)

Generally three types of phase function (PF) are considered: the specular, the diffusely reflecting (Lambert) sphere, and the lunar phase function. Each function is normalized to unity over all solid angle.

The specular sphere radiates equally into $4\pi$ steradians independent of phase angle ($\phi_P$ = angular separation between the source and the observer with the object at the vertex) and thus its phase function is simply:

$$PF_S = \frac{1}{4\pi} \quad \text{(AA.w)}$$

The Lambert phase function is a diffuse radiator with a maximum in the backscatter direction ($\phi_P$ = 0) and a minimum in the forward scattering direction ($\phi_P = \pi$). The

functional relationship is given by:

$$PF_L = \frac{2}{3\pi^2}\left[\sin(\phi_P) + (\pi - \phi_P)\cdot\cos(\phi_P)\right] \qquad \text{(AA.x)}$$

The lunar phase function is empirically derived from lunar observations (Allen 1973). It has a very strong backscatter component ($\phi_P$=0) and can be approximated in the range (40<$\phi_P$<110 degrees) as (Mulrooney 1993):

$$PF_M = \frac{5}{\pi^2}\left[5.3095x10^{-5}\cdot(\phi_P)^2 - 1.2591x10^{-2}\cdot\phi_P + 0.79121\right] \qquad \text{(AA.y)}$$

The phase function for orbital objects can generally be approximated by linear combinations of these three functions with most objects characterized by the specular and Lambert functions.

Figure AA-1 illustrates the functional behavior of these three phase functions as well as that of the lunar quadratic approximation.

Since most orbital object observations are made at solar phase angles between 40 and 100 degrees, we consider for this example a Lambert sphere at $\phi_P = \frac{\pi}{2}$, therefore:

$PF_L$ =0.0675.

Normalized Specular, Lambert, Lunar, and Lunar Quadratic Phase Functions

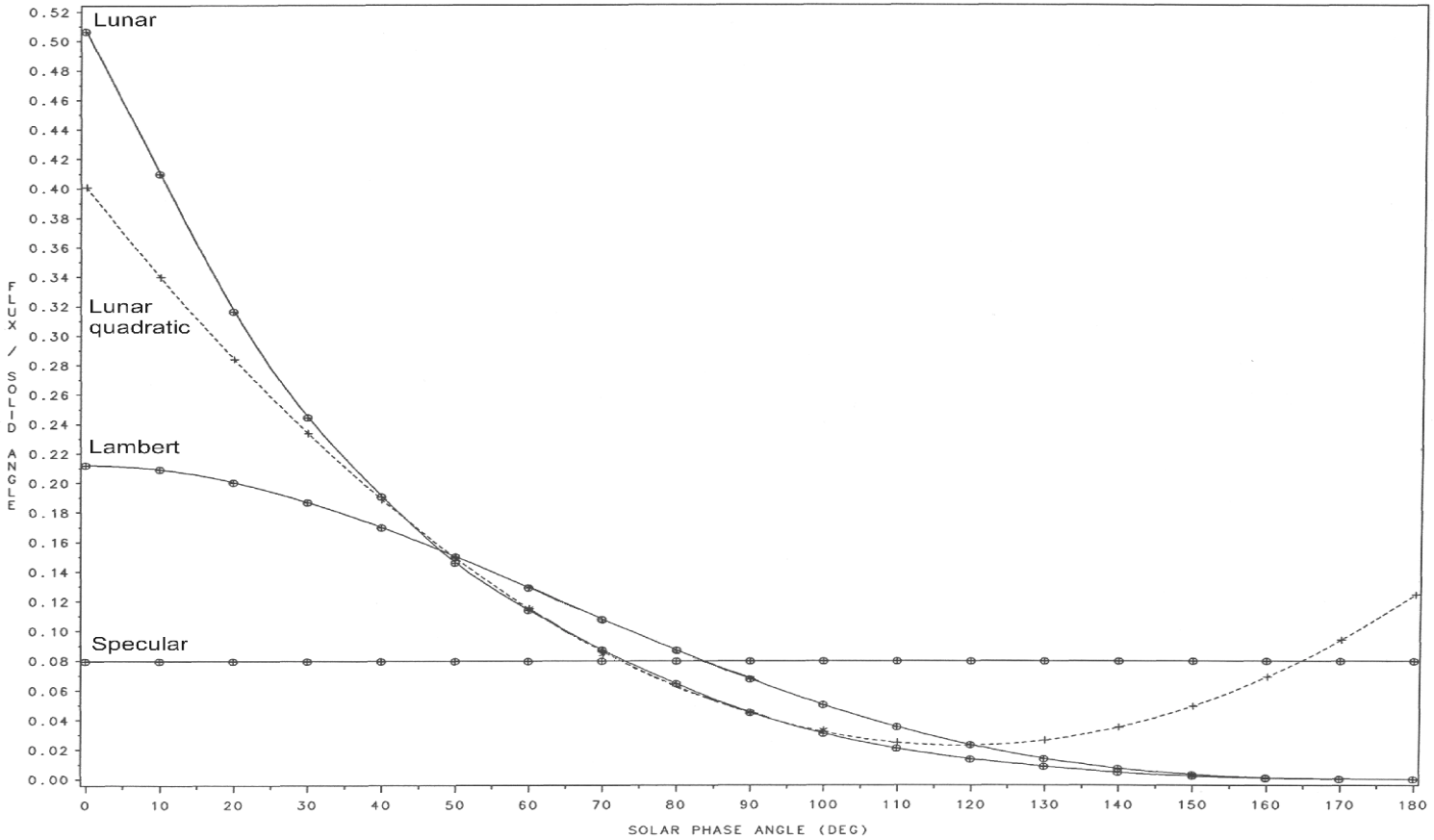


Figure AA-1. A graph demonstrating the three primary phase functions employed in orbital object research. (All are normalized to unity.) The strong backscatter behavior of the lunar function is evident as is the isotropic behavior of the specular sphere. The quadratic approximation to the lunar function fits well in the critical (solar phase angle= 40-100 deg) regime where most optical observations are made. The phase functions of most orbital objects can be approximated by a linear combination of the specular and Lambert functions. (Mulrooney 1993)

Substituting all known values into equation (AA.v) and solving for D:

D = 0.910 cm

Thus ideally, the NASA-LMT can detect an orbital object of 0.910 cm diameter while operating in the drift-matching (DM) mode in the V Band. In reality, this limiting diameter is not achieved, due to the additional noise contribution from background stars on the rapidly drift-scanning pixel. There is also a smearing effect which causes the signal photons to spread over several super-pixels with a consequent reduction in the SNR. This smearing is due to imperfect charge- transfer-efficiency (CTE) in the LSP 2K CCD, the discreet nature of the CCD parallel shifting relative to the continuous motion of the orbital object (or star) (Gibson and Hickson 1992b), and the inability to accurately set the CCD read rate to exactly match the angular velocity of high-speed motion. These limitations normally result in the signal occupying a minimum of 9 super-pixels with a significant loss in sensitivity. For an orbital object with identical properties to those in this example observed with the LSP 2K CCD, the empirical limiting diameter in DM mode is approximately 2.5 cm (Chapter II, Figure II.B-7).

# APPENDIX B

(NASA-LMT Orbital Object Detection in Drift Matching (DM) Mode)

```
      PROGRAM LMTTDI    FORTRAN 77
!     MARK MULROONEY V2.5

      CHARACTER*250 DCHR(100)

      INTEGER   OUTFILE
      REAL    DARK, DR, R, A, B, M2, EXPHLD, LRO
      REAL     BIN, RE, GM, PS, FW, PXA, SN, READ, SKY, PF, ALB
      REAL    NPIX, WS, WO, INC, ALPHA, RS, RO, RCM, D, PI, DU, DD
      REAL    SIGEXP, SOLMAG, NOISE, DELTR, DELTI, M1
      REAL     WOT, WEW, WNS, WEARTH, SITE, WST, WEWT, WNST, SI
      REAL    SIGEXPMX, EPSILON, EXPMX
      REAL          DATA(40,40)
      INTEGER       INCMX, RANMX, J1, INCMX1

      OUTFILE= 20

      OPEN (UNIT=OUTFILE,FILE='L8Mth.DAT',
      D.      STATUS='NEW', RECL=250, FORM='FORMATTED')

      SKY=22.0  !!  !MAG/"^2
      EXPMX=1800          ! LMT 16.O SKY -> 8000 E-/PIX-SEC  80K FullWell
!     3 SEC GIVES 50% DUTY CYCLE AT 2X2 BINNING
!     EXPMX=30    ! CDT MAUI 22.0 SKY -> 120 e-/PIX-S
      INCMX=17    ! 16# OF INC BINS
      RANMX=33   ! 33# OF RANGE BINS
      RS=850  !!     ! TDI OPTIMUM RANGE GEO39754 (range of desired obj)
      BIN=16          !!      ! 37K/20K-2 , 3500-4, 1500-8, 800-16  HOUSTON:>8
      DELTR=2  !!  ! GEO/20K-500, 3.5K-50, 1.5K/800-25 400-10
      DELTI=3   !!  ! INCLINATION INCREMENT 37K=1, all else 2
      SITE=0.0       ! SITE LATITUDE    (Use 0.0 for everything)
      SI=0.0          ! SEARCH INCLINATION  (Inc of desired object)
      PI=3.141592
      SOLMAG=-26.74

      WEARTH=0.004178 !ANG ROT EARTH IN 23:56
      GM=398666   !KM3/S2
      RE=6378               !KM
```

```
      PS=6040        !PIX/DEG   LMT
      FW=0.339       !DEG
      PXA=0.355      !"2/PIX
      READ=28.1      !e-/PIX
      DARK=0.0
      SN=6.31              !2MAG ABOVE NOISE
      PF=2/(3*PI**2)       !LAMBERT PF@90DEG  !SPHERE=1/4PI  (L<Specular)
!     PF=2/(PI**2)  !LAMBERT PF @ 15DEG
      ALB=0.1
!     PS=313               !PIX/DEG   CDT
!     FW=1.84
!     PXA=132
!     READ=100
!     DARK=50

      R=READ
      DR=DARK

      ALPHA=5.5135E+10  !10,000 P/SEC-CM^2 NM*MIRRORA*BW*THROUGH*QE
!     ALPHA=5.702E+8       !CDT
      A=ALPHA

      DATA(2,1)=0

      DO I=1,INCMX
      DATA(I+2,1)=I*DELTI
      END DO

      DO J=1,RANMX
!     RO=(RS-DELTR*((RANMX-1)/2))+DELTR*(J-1)
      RO=250*(1.191**(J-1))
      LRO=LOG10(RO)
      DATA(2,J+1)=LRO
      END DO

      DO I=1,INCMX
            DO J=1,RANMX

!           RO=(RS-DELTR*((RANMX-1)/2))+DELTR*(J-1)
!           RO=500+DELTR*(J-1)
            RO=250*(1.191**(J-1))
            INC=(I-1)*DELTI*PI/180
            RCM=RO*100000
```

```
                WST=(180/PI)*(GM/((RE+RS)*RS**2))**0.5
                WEWT=(WST*COS(SI))-WEARTH*COS(SITE)  ! ew motion of obj'
                WNST=WST*SIN(SI)
                WS=(WEWT**2+WNST**2)**0.5

                WOT=(180/PI)*(GM/((RE+RO)*RO**2))**0.5
                WEW=(WOT*COS(INC))-WEARTH*COS(SITE)
                WNS=WOT*SIN(INC)
                WO=(WEW**2+WNS**2)**0.5  ! Obj motion wrt telescope

                SIGEXP=FW/(WO*COS(INC))
                SIGEXPMX=SIGEXP
                EXP=FW/WS
                EXPHLD=EXP

                IF (EXP .GT. EXPMX) THEN
                        EXP=EXPMX
                ENDIF

                IF (WEW .LT. 0) THEN
                WO=-WO
                END IF

                EPSILON=(FW*PS/BIN)*(((WS/WO-1)**2+((TAN(INC-SI))**2))**0.5)
                NPIX=1+EPSILON

                IF (SIGEXP .GT. EXPMX) THEN
                        SIGEXP=EXPMX
                        NPIX=1+EPSILON*(EXPMX/SIGEXPMX)
                ENDIF

                B=BIN**2
                NOISE=((R**2)+(DR*EXP*B)+A*PXA*B*EXP*(10**-0.4*SKY))**0.5
                M1=-2.5*LOG10(SN*(NPIX**0.5)*NOISE/(ALPHA*SIGEXP))
                M2=M1-1.0    ! Accounts for 6 pix image spread

                DU=RCM*(10**(0.2*(SOLMAG-M2)))
                DD=((ALB*PI*PF/4)**0.5)
                D=DU/DD

        DU=RCM*(10**(SOLMAG/5))*(SN**0.5)*(NPIX**0.25)*(NOISE**0.5)
!               DD=((ALPHA*SIGEXP*ALB*PI*PF/4)**0.5)
                DATA(I+2,J+1)=M1
```

```
!               WRITE(*,*)DATA(I,J)
                WRITE(*,*) RO,INC
                WRITE(*,*) EXP, SIGEXP, EXPHLD, BIN
                WRITE(*,*) WO, WS, D, M1, NPIX


                END DO
        END DO

!       WRITE(*,*) EXP

        INCMX1=INCMX-1
        DCHR(1)(1:250)=' '
        DCHR(2)(1:250)=' '
        WRITE(UNIT=DCHR(1)(1:7),FMT='(I6)') INCMX1
        WRITE(UNIT=DCHR(1)(8:14),FMT='(I6)') RANMX

        DO J=1, RANMX
        J1=J-1
        WRITE (UNIT=DCHR(2)(1+J1*7:7+J1*7),FMT='(F7.2)') DATA(2,J)
        END DO

        DO I=3, INCMX

        DCHR(I)(1:250)=' '

        DO J=1, RANMX

        J1=J-1

        WRITE (UNIT=DCHR(I)(1+J1*7:7+J1*7),FMT='(F6.1)')DATA(I,J)

        END DO
        END DO


        DO I=1,INCMX

        WRITE(20,200) DCHR(I)
        FORMAT(A250)

        END DO
        END
```

# APPENDIX C1

## (Original 3 Element Corrector Parameter File)

(Values in parentheses are manufactured values)

```
3-m POTTER TEL CORRECTOR, Radii from APS Tooling List; 60 mm field.
STOP IS SURF  2
IMAGE IS 11
PXRAY      0.1500000E+04  0.1477440E+17  0.5760000E-02  0.2659392E+02
WVLNS.  0.5000000E+03  0.4000000E+03  0.8000000E+03  0.6000000E+03
            0.7000000E+03

 1  0 CURVATURE DATA          0.0000000E+00  0.0000000E+00  0.0000000E+00
 2  0 AXIAL SEPARATION       -0.2565000E+19
 3  0 AIRSPACE


 1  1 CURVATURE DATA          0.0000000E+00  0.0000000E+00  0.0000000E+00
 2  1 AXIAL SEPARATION       -0.4617000E+04
 3  1 AIRSPACE


 1  2 CURVATURE DATA          0.1112664E-03  0.8987439E+04 –0.1000000E+01
 2  2 AXIAL SEPARATION        0.4048655E+04
 3  2 REFLECTING SURF.       –0.1000000E+01 –0.1000000E+01 –0.1000000E+01
                             -0.1000000E+01 –0.1000000E+01
 4  2 TILT ANGLES- 123        0.0000000E+00  0.0000000E+00  0.0000000E+00


 1  3 RADIUS DATA             0.5000000E-02  0.2000000E+03  0.0000000E+00
                                                (0.19967E+3)
 2  3 AXIAL SEPARATION        0.2400000E+02
                             (0.2422E+02)
 3  3 INDICES                -0.1521415E+01 –0.1530852E+01 –0.1510779E+01
                             -0.1516294E+01 –0.1513065E+01
 3  3 ABBE NUMBER =   64.13 Glass type BK7      (64.2)


 1  4 RADIUS DATA             0.4945598E-02  0.2022000E+03  0.0000000E+00
                                                (0.202575E+03)
```

2 4 AXIAL SEPARATION 0.2408604E+03
3 4 AIRSPACE

1 5 RADIUS DATA 0.2689618E-02 0.3718000E+03 0.0000000E+00
(0.37192E+03)
2 5 AXIAL SEPARATION 0.3920000E+02
(0.39115E+02)
3 5 INDICES -0.1521415E+01 –0.1530852E+01 –0.1510779E+01
-0.1516294E+01 –0.1513065E+01
3 5 ABBE NUMBER = 64.13 Glass type BK7 (64.2)

1 6 RADIUS DATA 0.1171783E-01 0.8534000E+02 0.0000000E+00
(0.8541E+02)
2 6 AXIAL SEPARATION 0.1004035E+03
3 6 AIRSPACE

1 7 RADIUS DATA 0.6995453E-02 0.1429500E+03 0.0000000E+00
(0.143034E+03)
2 7 AXIAL SEPARATION 0.1570000E+02
(0.1576E+02)
3 7 INDICES -0.1521415E+01 –0.1530852E+01 –0.1510779E+01
-0.1516294E+01 –0.1513065E+01
3 7 ABBE NUMBER = 64.13 Glass type BK7 (64.2)

1 8 RADIUS DATA -0.2834467E-02 –0.3528000E+03 0.0000000E+00
(0.3527E+03)
2 8 AXIAL SEPARATION 0.3680925E+02
3 8 AIRSPACE

1 9 CURVATURE DATA 0.0000000E+00 0.0000000E+00 0.0000000E+00
2 9 AXIAL SEPARATION 0.3175000E+01
3 9 INDICES -0.1462319E+01 –0.1470114E+01 –0.1453310E+01
-0.1458035E+01 –0.1455289E+01
3 9 ABBE NUMBER = 67.86 Glass type FS (67.8)

1 10 CURVATURE DATA 0.0000000E+00 0.0000000E+00 0.0000000E+00
2 10 AXIAL SEPARATION 0.9525000E+01
3 10 AIRSPACE

1 11 CURVATURE DATA 0.0000000E+00 0.0000000E+00 0.0000000E+00

potopt500.out

centroid for all rays : 0.0000 -0.0011

colours : 400.00 500.00 650.00 800.00 1000.00

y offsets for each height, colour

| | | | | | |
|---|---|---|---|---|---|
| D.1 | 0.0110 | 0.0101 | 0.0082 | 0.0067 | 0.0050 |
| 18.49 | –0.0056 | –0.0045 | –0.0044 | –0.0046 | –0.0050 |
| 15.05 | –0.0061 | –0.0049 | –0.0047 | –0.0048 | –0.0050 |
| 7.50 | –0.0040 | –0.0033 | –0.0031 | –0.0031 | –0.0031 |
| D.1 | 0.0000 | 0.0000 | 0.0000 | 0.0000 | 0.0000 |

Maximum spot diameter = 0.14419431468227

Maximum spot sizes ...

| | | | | |
|---|---|---|---|---|
| D.1 | 0.0636 | 0.0827 | 0.0914 | 0.0980 |
| D.1 | 0.1258 | 0.1176 | 0.1150 | 0.1140 |
| D.1 | 0.1073 | 0.1030 | 0.1025 | 0.1033 |
| D.1 | 0.0494 | 0.0528 | 0.0565 | 0.0608 |
| D.1 | 0.0061 | 0.0105 | 0.0180 | 0.0257 |

80 percent-energy spot sizes ...

| | | | | |
|---|---|---|---|---|
| D.1 | 0.0333 | 0.0447 | 0.0512 | 0.0576 |
| D.1 | 0.0292 | 0.0236 | 0.0229 | 0.0246 |
| D.1 | 0.0257 | 0.0189 | 0.0182 | 0.0202 |
| D.1 | 0.0143 | 0.0077 | 0.0090 | 0.0113 |
| D.1 | 0.0047 | 0.0055 | 0.0068 | 0.0080 |

Half-energy spot sizes ...

| | | | | |
|---|---|---|---|---|
| D.1 | 0.0211 | 0.0252 | 0.0283 | 0.0318 |
| D.1 | 0.0153 | 0.0103 | 0.0110 | 0.0129 |
| D.1 | 0.0136 | 0.0093 | 0.0095 | 0.0114 |
| D.1 | 0.0078 | 0.0056 | 0.0046 | 0.0061 |
| D.1 | 0.0037 | 0.0036 | 0.0052 | 0.0068 |

total number of rays = 9646

# APPENDIX C2

## (Modified 4 Element Corrector Parameter File)

07/11/97

NASA-LMT
Modification to the existing 3 Element Wynne Corrector
Elements 1 and 2 retained
Elements 3 and 4 new

System saved in file CONBK.LEN(5)
CODE V> lis
LMT, 4-el, 3rd aspheric

| | RDY | THI | RMD | GLA | CCY | THC | GLC |
|---|---|---|---|---|---|---|---|
| OBJ: | INFINITY | INFINITY | | | 100 | 100 | |
| STO: | -8988.14679 | -4045.616841 | REFL | | | 0 | 100 |
| CON: | | | | | | | |
| K : | -1.000000 | KC : | 100 | | | | |
| 2: | -199.67000 | -24.220000 | | BK7_SCHOTT (old) | 100 | 100 | |
| 3: | -202.57500 | -240.860400 | | AIR | 100 | 100 | |
| 4: | -371.92000 | -39.115000 | | BK7_SCHOTT (old) | 100 | 100 | |
| 5: | -85.41000 | -66.694774 | | AIR | 100 | 0 | |
| 6: | -77.86514 | -10.000000 | | BK7_SCHOTT (new) | 0 | 0 | |
| 7: | -66.04087 | -33.063174 | | AIR | 0 | 0 | |
| CON: | | | | | | | |
| K : | -0.371270 | KC : | 0 | | | | |
| 8: | -70.08598 | -18.518725 | | BK7_SCHOTT (new) | 0 | 0 | |
| 9: | -313.45086 | -18.422555 | | AIR | 0 | 0 | |
| 10: | INFINITY | -7.000000 | | ‘gg455’ | 100 | 100 | |
| 11: | INFINITY | -5.000000 | | | 100 | 100 | |
| 12: | INFINITY | -3.175000 | | SILICA_SPECIAL | 100 | 100 | |
| 13: | INFINITY | -9.525000 | | | 100 | 100 | |
| IMG: | INFINITY | 0.000000 | | | 100 | 100 | |

SPECIFICATION DATA

| | | | | | |
|---|---|---|---|---|---|
| EPD | 2999.99986 | | | | |
| DIM | MM | | | | |
| WL | 1000.00 | 800.00 | 600.00 | 500.00 | 400.00 |
| REF | 3 | | | | |
| WTW | 1 | 1 | 1 | 1 | 1 |
| INI | her | | | | |
| XAN | 0.00000 | 0.00000 | 0.00000 | 0.00000 | 0.00000 |
| | 0.00000 | | | | |
| YAN | 0.00000 | 0.08000 | 0.16000 | 0.22400 | 0.32000 |
| | -0.32000 | | | | |

APERTURE DATA/EDGE DEFINITIONS

| | | |
|---|---|---|
| CA | | |
| CIR S1 | | 1500.000000 |
| CIR S2 | | 148.000000 |
| CIR S4 | | 70.000000 |
| CIR S6 | | 53.500000 |
| CIR S7 | | 53.500000 |
| CIR S8 | | 48.500000 |
| CIR S9 | | 48.500000 |
| CIR S2 | EDG | 148.000000 |
| CIR S4 | EDG | 70.000000 |
| CIR S6 | EDG | 53.500000+-0.1 mm |
| CIR S7 | EDG | 53.500000+-0.1 mm w/ 4.5mm Land |
| CIR S8 | EDG | 48.500000+-0.1 mm |
| CIR S9 | EDG | 48.500000+-0.1 mm w/ 3.5mm Land (if necessary) |

PRIVATE CATALOG

| | | | |
|---|---|---|---|
| PWL | 1014.00 | 587.60 | 480.00 |
| ‘gg455’ | 1.530000 | 1.540000 | 1.550000 |

REFRACTIVE INDICES

| GLASS CODE | 1000.00 | 800.00 | 600.00 | 500.00 | 400.00 |
|---|---|---|---|---|---|
| BK7_SCHOTT | 1.507502 | 1.510776 | 1.516295 | 1.521414 | 1.530849 |
| SILICA_SPECIAL | 1.450416 | 1.453318 | 1.458041 | 1.462331 | 1.470122 |
| ‘gg455’ | 1.530130 | 1.532831 | 1.539300 | 1.547361 | 1.569763 |

INFINITE CONJUGATES
EFL -5152.9216
BFL -9.5684
FFL 50653.7178
FNO 1.7176
IMG DIS -9.5250
OAL -4511.6865
PARAXIAL IMAGE
HT 28.7796
ANG 0.3200
ENTRANCE PUPIL
DIA 2999.9999
THI 0.0000
EXIT PUPIL
DIA 305.1852
THI -533.7669

APPENDIX D

Galaxy Distribution/Clustering for a R.A. and Declination Wedge to z = 0.033

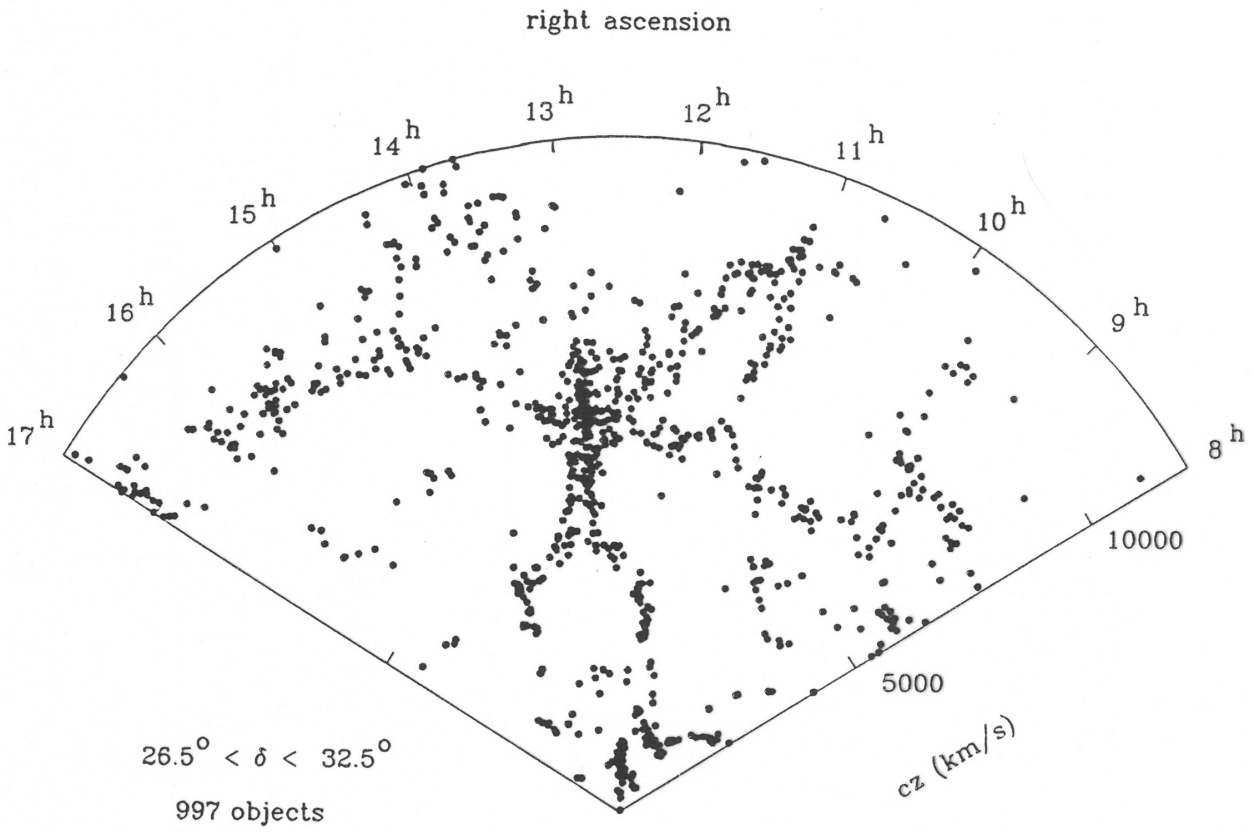


Figure AD-1. A two dimensional representation of a R.A. and Declination wedge showing the distribution of galaxies to z = 0.033. Galaxy clustering is clearly evident. The UBC/NASA-LMT multi-narrowband survey will generate a similar figure, but extending 15 times deeper in z (0.5), over 12-18 hr R.A. and +-16 arcminute declination range centered on +32.979 degrees. (Figure credit: de Lapparent et al. 1986).

# APPENDIX E

## B Band Filter Transmission

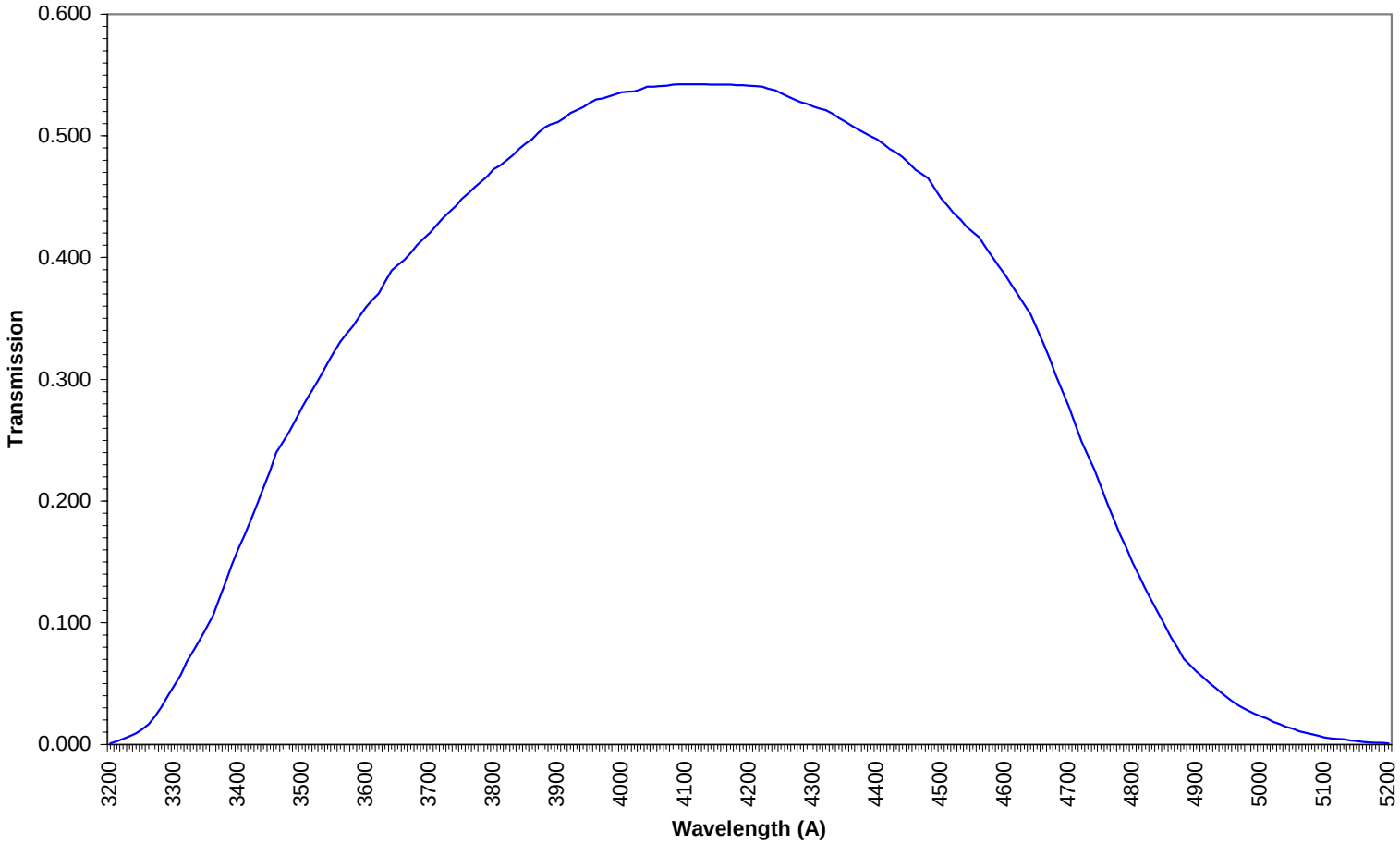


Figure AE-1. Measured broadband transmission for the UBC/NASA B Band filter.

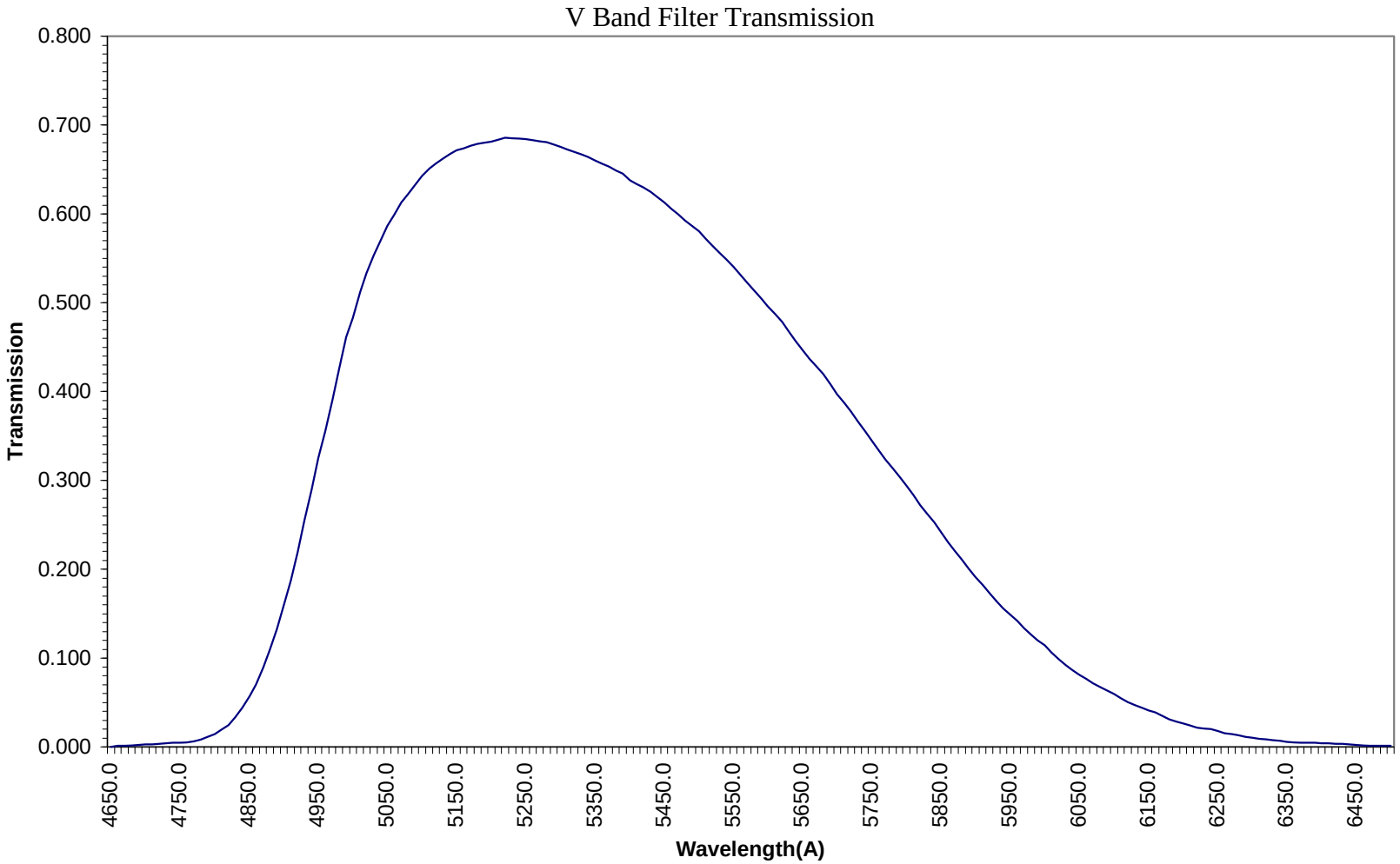


Figure AE-2. Measured broadband transmission for the UBC/NASA V Band filter.

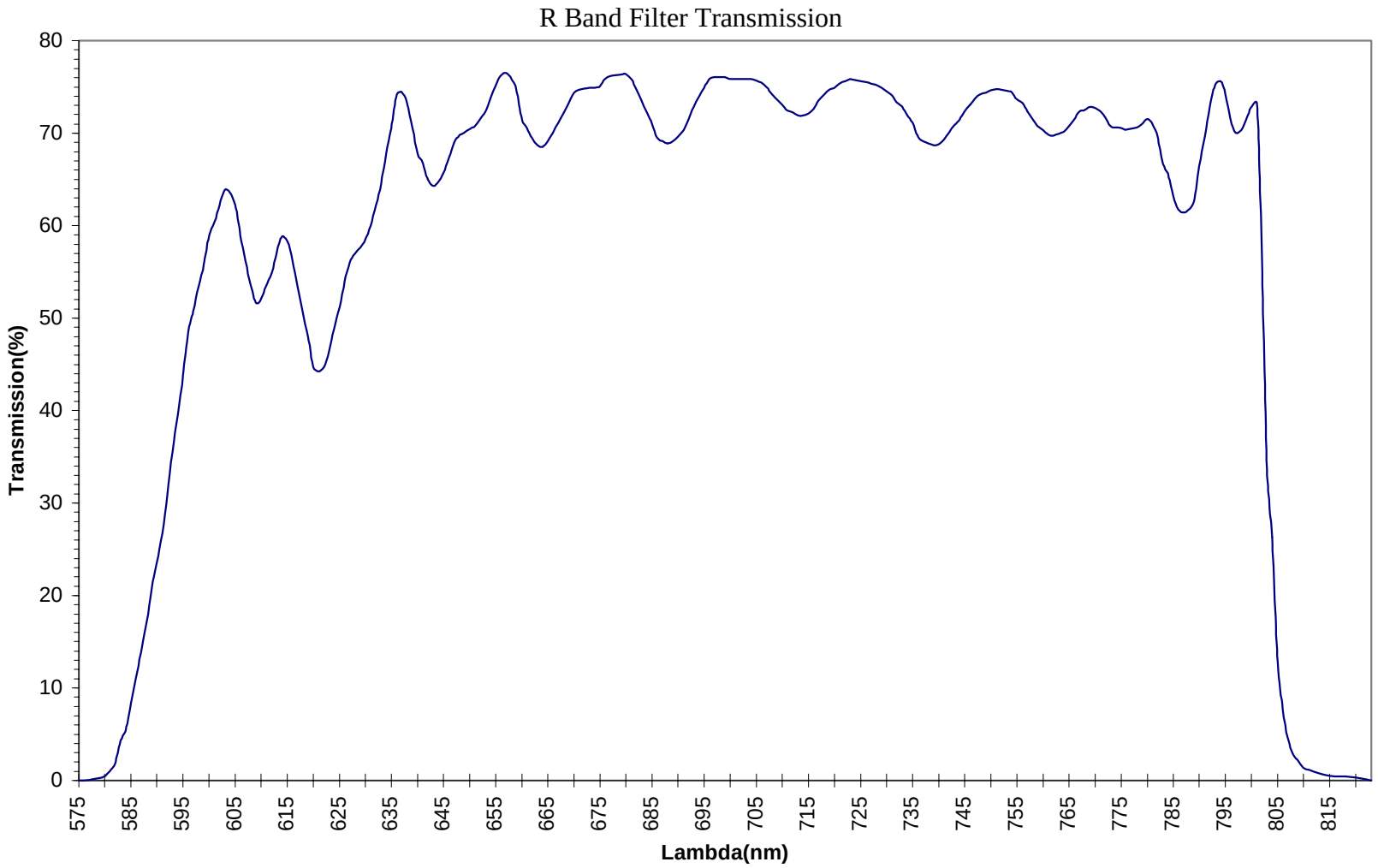


Figure AE-3. Measured broadband transmission for the UBC/NASA R Band filter.

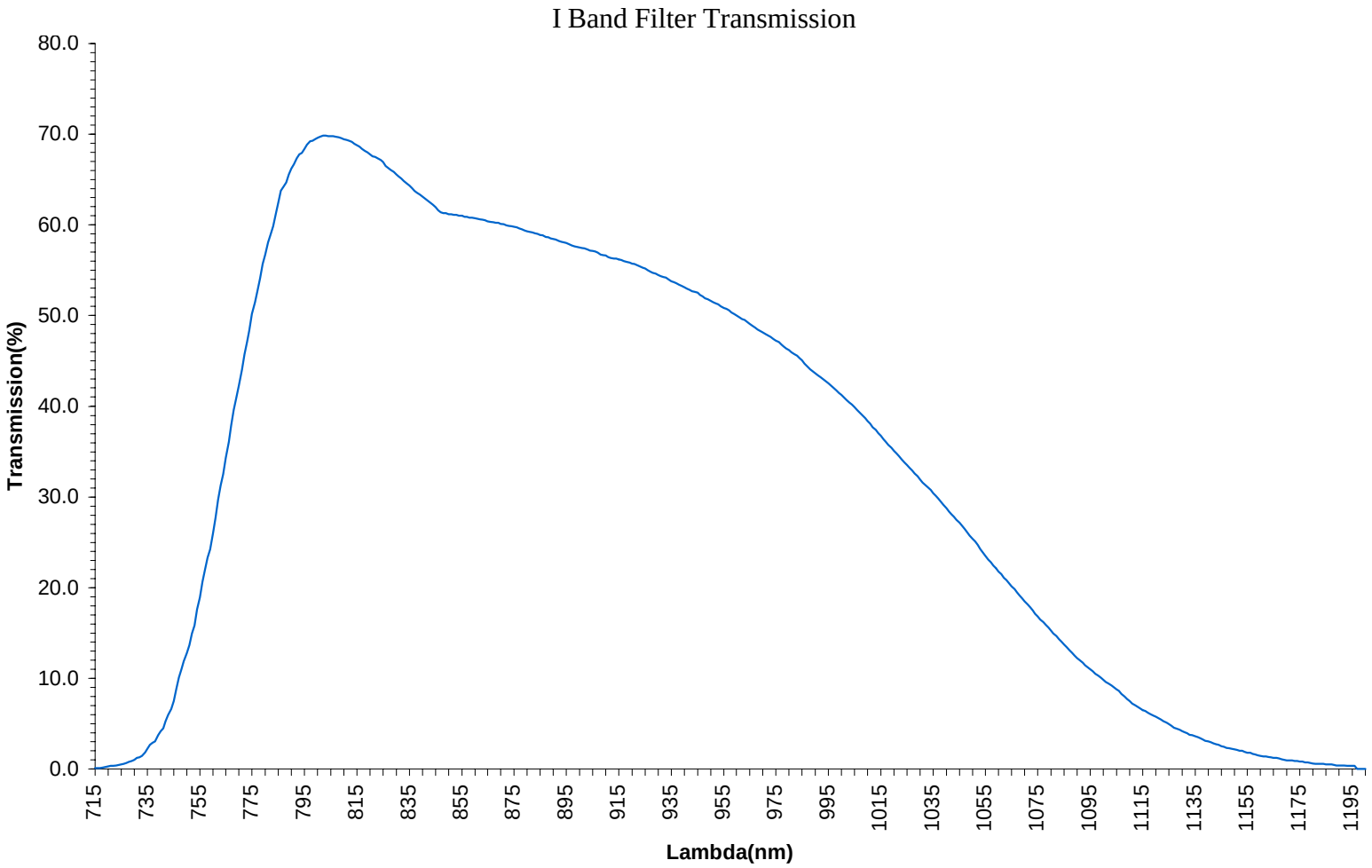


Figure AE-4. Measured broadband transmission for the UBC/NASA I Band filter.

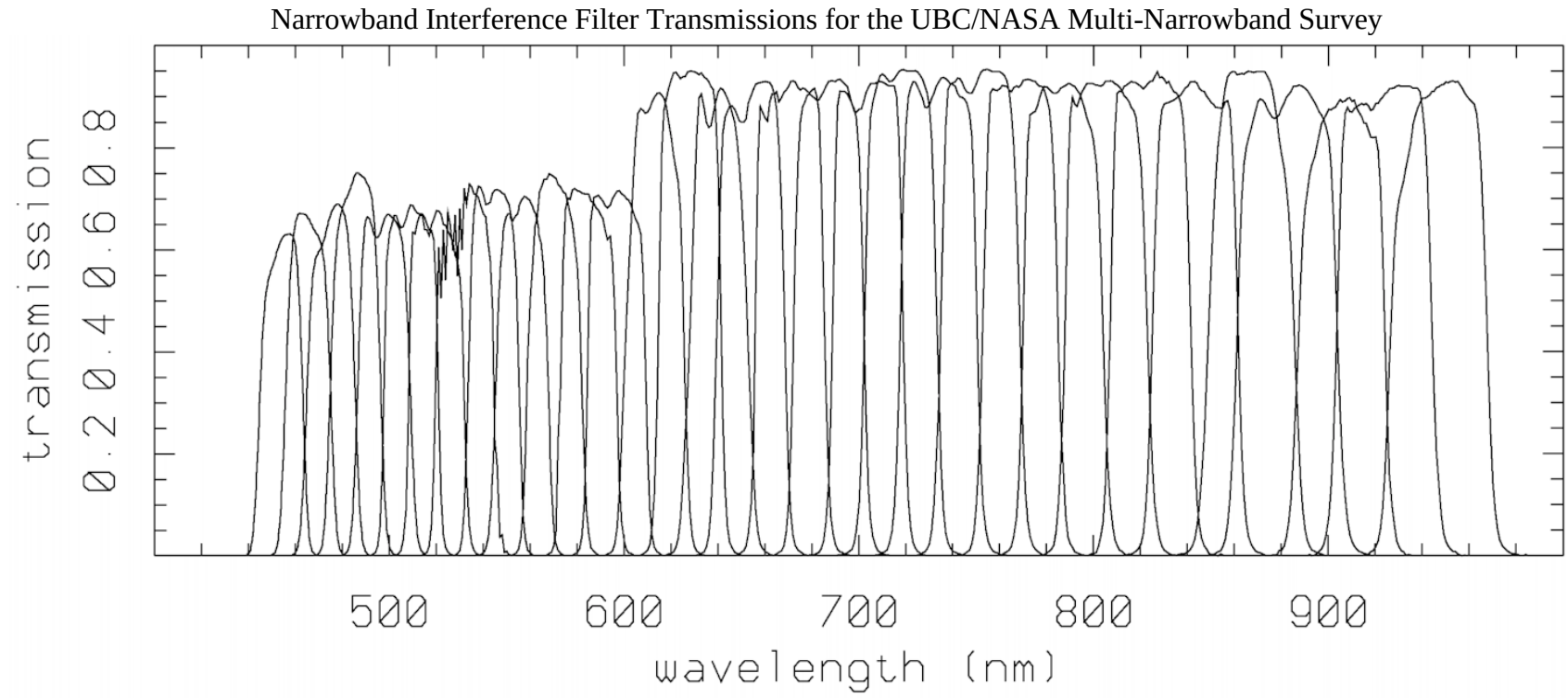


Figure AE-5. Transmissions for the 40 narrowband interference filters used in the UBC/NASA Multi-Narrowband Survey. The filters are spaced equally in log frequency and have equal energy bandpasses at all frequencies. Used together they can yield photometric redshifts (z) with +- 0.02 accuracy.